# Analysis of the bifurcation diagram of a hybrid bistable system with feedback controls of chaos

Zhi-Ren Zheng,* Jian Huang, and Jin-Yue Gao
*Physics Department, Jilin University, Changchun, Jilin 130023, China*
(Received 25 March 1999)

Based on the dynamic equation of a hybrid bistable system with a delayed feedback, we have studied changes of the bifurcation diagram of its output oscillation under chaos suppression and delayed feedback control of chaos, respectively, and the physical origin of these changes. The result clearly shows that, in this case, the input intensity of the system is replaced by a smaller effective input intensity. So the bifurcation diagram is shifted to its right side, and a certain part of the chaotic oscillation becomes periodic oscillation. [S1063-651X(99)07811-3]

PACS number(s): 05.45.Gg, 42.65.Sf

## I. INTRODUCTION

The chaos suppression (CS), $F(t)=X[-V(t)]$, proposed by Davis [1], and the delayed feedback control of chaos (DFC), $F(t)=X[V(t-T)-V(t)]$, proposed by Pyragas [2], are two effective and convenient methods of chaos control. The latter one has been successfully applied to many systems [3–10]. Using these two methods, we have realized the feedback control of chaos theoretically and experimentally in an electro-optical bistable system with a delayed feedback, and successfully demonstrated the dynamic storage function of the system [11]. In the meantime, we have found that, following these feedback controls, the whole bifurcation diagram is shifted to its right side.

In this paper we will discuss the changes of the bifurcation diagram under CS and DFC, respectively, and explore the physical nature of the process from the viewpoint of bifurcation diagram analysis and give a theoretical understanding for the feedback controls of chaos in a hybrid bistable system with a delayed feedback.

## II. THE CHANGES OF THE BIFURCATION DIAGRAM UNDER THE FEEDBACK CONTROLS OF CHAOS

The dynamic behavior of a hybrid bistable system with a delayed feedback can be described by the following dimensionless equation [11,12]:

$$\frac{dV(t)}{dt}+V(t)=If(V(t-\tau)), \tag{1}$$

where $I$ and $V(t)$ represent the input and output intensities, respectively. $\tau$ is the effective delay time in the feedback loop. Both $\tau$ and the effective time variable $t$ are scaled to the natural response time of the system.

Applying CS or DFC to the above system, then performing numerical simulation for an electro-optical bistable system with a delay, we get the following dynamic equation with the chaos suppression or the chaos control:

$$\frac{dV(t)}{dt}+V(t)=If(t)+F(t), \tag{2}$$

where $F(t)=X[-V(t)]$ (CS) or $X[V(t-T)-V(t)]$ (DFC), $X$ is the weight of the chaos suppression or the chaos control, $T$ is the effective delay time of chaos control and also scaled to the natural response time of the system; $f(t)=0.5(1-K\cos[V(t-\tau)+\theta)]$, while $K$ is the extinction coefficient of the electro-optical bistable system and $\theta$ is the initial phase of the system [11].

First, let us study the change of the bifurcation diagram under a CS. Setting the control term $F(t)$ to be $X[-V(t)]$, the weight $X$ to be $-0.2$, 0.0, 0.2, respectively, and the delay time $\tau$ of the system to be 20.0, we solve Eq. (2) with Runge-Kutta method and get three corresponding bifurcation diagrams of the output oscillation level $V_p$ with a long delay of the system, as shown in Fig. 1. Figure 1(a) is the bifurcation diagram in the absence of chaos suppression. Comparing Fig. 1(b), which corresponds to $X=-0.2$, with Fig. 1(a), we find that the whole bifurcation diagram is shifted and compressed to the left side. In this case, part of the periodic oscillation region in Fig. 1(a) now lies in the chaotic oscil-

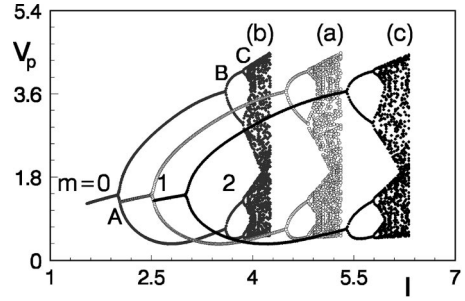


FIG. 1. The output oscillation level $V_p$ as a function of input intensity $I$. The parameters: $K=0.8$, $\theta=\pi$, $\tau=20.0$, $F(t)=X[-V(t)]$; (a) $X=0.0$, without any chaos suppression; (b) $X=-0.2$, with a CS; (c) $X=0.2$, with a CS. The points $A$, $B$, and $C$ in 1(b) indicate the first, the second, and the third bifurcation points, respectively. The bifurcation orders $m=0$, 1, and 2 in 1(b) indicate the bifurcation regions before the bifurcation point $A$, between the bifurcation points $A$ and $B$, and between the bifurcation points $B$ and $C$, respectively.

*Electronic address: qol@mail.jlu.edu.cn

 

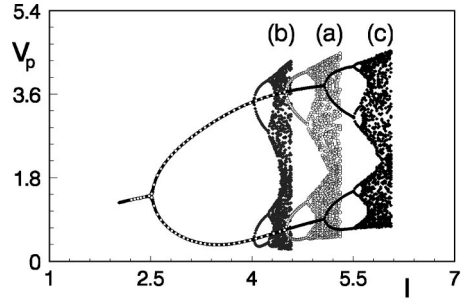


FIG. 2. The output oscillation level $V_p$ as a function of input intensity I. The parameters: $K=0.8$, $\theta=\pi$, $\tau=20.0$, $F(t)=X[V(t-2\tau)-V(t)]$; (a) $X=0.0$, without any chaos control; (b) $X=-0.2$, with a DFC; (c) $X=0.2$, with a DFC.

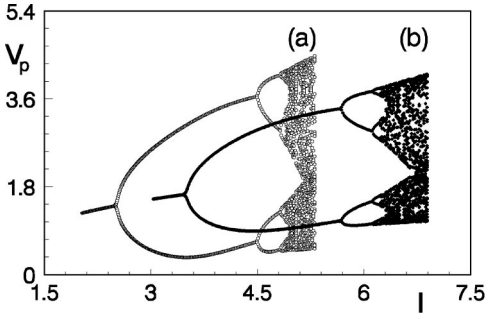


FIG. 3. The output oscillation level $V_p$ as a function of input intensity I. The parameters: $K=0.8$, $\theta=\pi$, $\tau=20.0$, $F(t)=X[V(t-\tau)-V(t)]$; (a) $X=0.0$, without any chaos control; (b) $X=0.2$, with a DFC.

lation region in Fig. 1(b). By comparing Fig. 1(c), which corresponds to $X=0.2$, with Fig. 1(a), we find that the whole bifurcation diagram is shifted and lengthened to the right side. In this case, part of the chaotic oscillation in Fig. 1(a) becomes the periodic oscillation in Fig. 1(c). So some chaotic states of the system can be suppressed by the CS of $X=0.2$.

Then, let us move to the case of DFC. Setting the control term F(t) to be $X[V(t-T)-V(t)]$, the weight $X$ to be $-0.2$, 0.0, 0.2, respectively, the delay time $\tau$ of the system to be 20.0, and the delay time $T$ of chaos control to be $2\tau$, as in the case of CS, we draw three corresponding bifurcation diagrams with a long delay of the system, as shown in Fig. 2. The comparison of Fig. 2(b), which corresponds to $X=-0.2$, and Fig. 2(a), which is the bifurcation diagram without any chaos control, shows that the steady state region of order $m=0$ (see Fig. 1) and the periodic oscillation region of order $m=1$ in Fig. 2(b) happen to coincide exactly with the corresponding parts in Fig. 2(a), and the bifurcation diagram is compressed to the left side. Instead of controlling chaos, such a feedback control enlarges the chaotic oscillation region of the system. But the comparison of Fig. 2(c), which corresponds to $X=0.2$, and Fig. 2(a) shows that the steady state region of $m=0$ and the periodic oscillation region of $m=1$ in Fig. 2(a) happen to coincide exactly with the corresponding parts in Fig. 2(c), and the bifurcation diagram is lengthened to the right side. Such a feedback control of chaos enlarges the periodic oscillation region of the system, so some chaotic states of the system can be controlled by the DFC of $X=0.2$ and $T=2\tau$.

In another case of DFC, setting the control term $F(t)$ to be $X[V(t-T)-V(t)]$, the weight $X$ to be 0.0 and 0.2, respectively, the delay time $\tau$ of the system to be 20.0, the delay time $T$ of chaos control to be $\tau$ instead of $2\tau$, and following the above process, we draw two corresponding bifurcation diagrams with a long delay of the system, as shown in Fig. 3. By comparing Fig. 3(b), which corresponds to $X=0.2$, with Fig. 3(a), which is the bifurcation diagram in the absence of chaos control, we find that the whole bifurcation diagram is shifted and lengthened to the right side. In this case, part of the chaotic oscillation in Fig. 3(a) becomes the periodic oscillation in Fig. 3(b), so some chaotic states of the system can also be controlled by the DFC of $X=0.2$ and $T=\tau$.

## III. THE PHYSICAL ORIGIN OF THE CHANGES OF THE BIFURCATION DIAGRAM

In order to find out the physical origin leading to the change of the bifurcation diagram, we substitute $F(t)=X[-V(t)]$ and $F(t)=X[V(t-T)-V(t)]$ into Eq. (2), then obtain the following differential equations for CS and DFC, respectively:

$$\frac{1}{1+X}\frac{dV(t)}{dt}+V(t)=I^*f(t), \tag{3}$$

$$\frac{1}{1+X}\frac{dV(t)}{dt}+V(t)=\frac{X}{1+X}V(t-T)+I^*f(t), \tag{4}$$

where $I^*=I/(1+X)$ is a new parameter and defined as an effective input intensity of the system.

Equations (3) and (4) clearly show that the input intensity $I$ in the dominant term $If(t)$ of Eq. (2) is replaced by an effective input intensity $I^*$ because of the feedback controls of chaos, so the whole bifurcation diagram of the system can be changed.

When the delay time $\tau$ of the system is long, the linear stability analysis shows that the odd harmonics of the eigen fundamental frequency of the system coincide with the corresponding higher eigenfrequencies of the system and are very strong while the even harmonics of the eigen fundamental frequency are far from the corresponding higher eigen frequencies and are very weak [13]. So the output oscillation is of square wave form and there is $dV(t)/dt\approx 0$ [11], and Eq. (3) can be approximated to the following iterative Equation:

$$V(t)=\frac{I}{1+X}f(t)=I^*f(t). \tag{5}$$

It is obvious that, with a negative CS of $X=0.2$, the effective input intensity is $(1+X)$ times less than the actual input intensity. Therefore each point on the bifurcation diagram in Fig. 1(a) is shifted from I to $(1+X)I$, and the bifurcation diagram is lengthened to the right side $(1+X)$ times as long as that of before chaos suppression. When a positive CS of $X=-0.2$ is applied to the system, the result is right on the contrary, as shown in Fig. 1(b).

When the delay time $\tau$ of the system is long, numerical simulation shows that the result calculated according to the

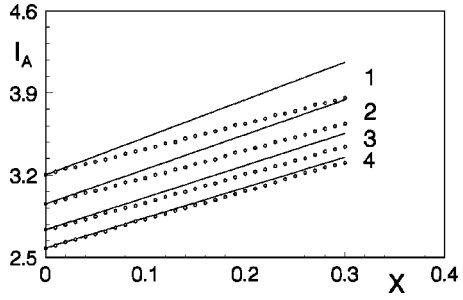


FIG. 4. The input intensity $I_A$ corresponding to the first bifurcation point A as a function of the weight $X$ of CS. The parameters: $K=0.8$, $\theta=\pi$, $F(t)=X[-V(t)]$. The curves composed of open circles are calculated from Eq. (3) when the delay time of the system is $\tau_i$ $(i=1-4)$, respectively. The solid lines represent the curves of $I_{Ai}=I_{0i}(1+X)(i=1-4)$ corresponding to the case of a long delay, where $I_{0i}$ $(i=1-4)$ are the input intensities corresponding to the first bifurcation point A, which are calculated from Eq. (3) when the weight $X$ equals zero and the delay time of the system is $\tau_i$ $(i=1-4)$, respectively. (1) $\tau_1=3.0$, $I_{01}=3.20$; (2) $\tau_2=4.0$, $I_{02}=2.96$; (3) $\tau_3=6.0$, $I_{03}=2.74$; (4) $\tau_4=10.0$, $I_{04}=2.58$.

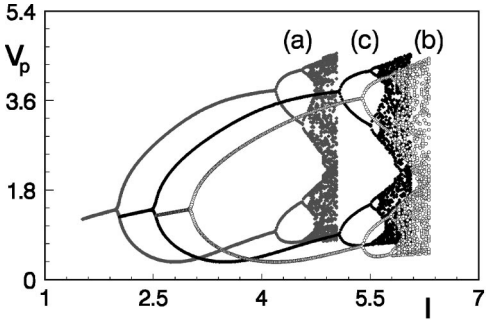


FIG. 5. The output oscillation level $V_p$ as a function of input intensity I. The parameters: $K=0.8$, $\theta=\pi$, $\tau=20.0$; (a) $F(t)=X[V(t-2\tau)]$, $X=0.2$, with a DFC; (b) $F(t)=X[-V(t)]$, $X=0.2$, with a CS; (c) $F(t)=X[V(t-2\tau)-V(t)]$, $X=0.2$, with a DFC.

differential equation (3) is the same as that calculated from the iterative equation (5). When the delay time $\tau$ of the system is short, the result calculated according to Eq. (3) qualitatively agrees with that calculated from Eq. (5), as we can see more clearly below.

With a negative CS and a short delay $\tau$ of the system, the shift behavior of the first bifurcation point A (see Fig. 1), which is calculated from Eq. (3), is shown in Fig. 4 (the open circles). With a negative CS and a long delay $\tau$ of the system, the regular pattern $I_A=I_0(1+X)$ of the shift of the same bifurcation point A, which is calculated from Eq. (5), is also shown in Fig. 4 (the solid lines). Figure 4 shows that the larger the weight $X$ of chaos suppression, the greater the shift of the first bufurcation point A. For the same weight $X$, Fig. 4 shows three features. First, the shift of the open circle line for a short delay is smaller than the corresponding shift of the solid line for a long delay. Second, the difference between the open circle line and the solid line for a shorter delay is larger than the difference for a longer delay. Third, with the increase of the delay time $\tau$, the difference quickly diminishes, and becomes very small when the delay time $\tau$ increases to 10.0 (curve 4).

Numerical simulation shows that, with a negative CS and a short delay $\tau$, the shift behavior of other points on the bifurcation diagram is the same as that of the first bifurcation point A.

Now, let us discuss the case of DFC. When the delay time $\tau$ of the system is long, there is $dV(t)/dt\approx 0$. So Eq. (4) can be approximated to the following iterative equation:

$$V(t)=\frac{X}{1+X}V(t-T)+\frac{I}{1+X}f(t)=\frac{X}{1+X}V(t-T)+I^*f(t). \tag{6}$$

The output oscillation for a long delay of the system is a typical square wave. So the period of the output oscillation is $2\tau$ in the bifurcation region of $m=1$, and $4\tau$ in the bifurcation region of $m=2$ [14].

When the delay time $T$ of chaos control is equal to the period $2\tau$ of the output oscillation in the bifurcation region of $m=1$, which is a typical choice for chaos control, and the weight $X$ of chaos control is equal to 0.2, for the bifurcation region before the second bifurcation point in Fig. 2(a), before and after the DFC, there is always $V(t\text{-}2\tau)=V(t)$, namely $F(t)=X[V(t-2\tau)-V(t)]=0$. Therefore Eq. (6) becomes $V(t)=If(t)$ within these regions, and the bifurcation regions of m=0 and 1 before the chaos control are not changed after the chaos control, as shown in the comparison of Figs. 2(a) and 2(c). But for the region after the second bifurcation point in Fig. 2(a), before the chaos control, $V(t-2\tau)$ is no longer equal to $V(t)$. Here the change of the bifurcation diagram is governed by the joint effect of the control terms $X[V(t-2\tau)]$ and $X[-V(t)]$. When only $X[V(t-2\tau)]$ is applied to the system, the bifurcation diagram is shifted and stretched to the left side, as shown in the comparison of Figs. 1(a) and 5(a). But when only $X[-V(t)]$ is applied to the system, the bifurcation diagram is shifted and lengthened to the right side, as shown in the comparison of Figs. 1(a) and 5(b), namely as shown in the comparison of Figs. 1(a) and 1(c). When $X[V(t-2\tau)-V(t)]$ is applied to the system, it is key that, under the feedback control of $X[-V(t)]$, the actual input intensity I in the dominant term $If(t)$ of Eq. (2) is replaced by a smaller effective input intensity $I^*=I/(1+X)$. In other words, here the effect of the control term $X[-V(t)]$ is stronger than the effect of the control term $X[V(t-2\tau)]$. So the region after the second bifurcation point in Fig. 2(a) is lengthened to the right side under the DFC of $X[V(t-2\tau)-V(t)]$, as shown in the comparison of Figs. 1(a) and 5(c), namely as shown in the comparison of Figs. 2(a) and 2(c). When the DFC of $X=-0.2$ is applied to the system and T is equal to $2\tau$, the result may be deduced by analogy, as shown in the comparison of Figs. 2(a) and 2(b).

Numerical simulation shows that, when the weight $X$ of chaos control is equal to 0.2, and the delay time $T$ of chaos control is set to be $4\tau$, for the bifurcation region before the third bifurcation point in Fig. 2(a), before and after the DFC, there is always $V(t-4\tau)=V(t)$. Therefore Eq. (6) becomes $V(t)=If(t)$ within these regions, the bifurcation regions of m=0, 1, and 2 before the chaos control are not changed after the chaos control, and the region after the third bifurcation

point in Fig. 2(a) is lengthened to the right side because of the joint effect discussed above.

If the delay time $\tau$ of the system is short, the eigen fundamental period of the output oscillation will not be equal to a multiple of $\tau$, for example $2\tau$ or $4\tau$. But if only the delay time $T$ of the chaos control is set to be the eigen fundamental period of the output oscillation of the system, we will also get the result similar to Fig. 2.

When the delay time $\tau$ of the system is long, the delay time $T$ of chaos control is equal to $\tau$, and the weight $X$ of chaos control is equal to 0.2, for the steady state region of $m=0$ in Fig. 3(a), before and after the DFC, there is always $V(t-\tau)=V(t)$. Therefore Eq. (6) becomes $V(t)=If(t)$ within this region, and the steady state region of $m=0$ before the chaos control coincides with the corresponding region of $m=0$ after the chaos control. For the bifurcation region of $m=1$ in Fig. 3(a), before the chaos control, $V(t-\tau)$ is no longer equal to $V(t)$. Setting $C_0=V(t-\tau)+V(t)$, where the parameter $C_0$ is a constant for a fixed input intensity $I$ and monotonically becomes larger along with the increase of the input intensity in the bifurcation region of m=1 in Fig. 3(a), then substituting $V(t-T)=V(t-\tau)=C_0-V(t)$ into Eq. (6), we get $V(t)=[C_0X/(1+2X)]+[I/(1+2X)]f(t)=[C_0X/(1+2X)]+I^*f(t)$. In this case, the effective input intensity of the system is $(1+2X)$ times less than the actual input intensity. The comparison between Figs. 3(b) and 3(a) shows that the first bifurcation point in Fig. 3(a) is shifted from $I$ almost to $(1+2X)I$, and the bifurcation diagram is also lengthened to the right side correspondingly, but the lengthened multiple is less than $(1+2X)$ because of the effect of the term $C_0X/(1+2X)$.

In conclusion, when a CS or a DFC is applied to a hybrid bistable system with a long delay, the input intensity can be replaced by a new effective input intensity. When the effective input intensity is smaller than the actual input intensity, the bifurcation diagram of the system is shifted to its right side, and part of the chaotic states of the system can become periodic states. As the delay time of the system becomes short, numerical simulation shows that the regularity of the change of the bifurcation diagram under the feedback controls of chaos gradually deviates from that with a long delay of the system, and the shorter the delay time, the larger the difference. Numerical simulation also shows that, with a short delay of the system, the result under DFC is more complicated than that under CS in general. This is because DFC is a joint effect of two control terms $X[V(t-T)]$ and $X[-V(t)]$, while CS is an effect of one control term $X[-V(t)]$ only. What one should notice is that the results in this paper are just from a hybrid bistable system with a delayed feedback, and it needs to be investigated further whether these results may be applied to other systems, especially the systems with a markedly different nature from the present one.


[1] P. Davis, Jpn. J. Appl. Phys., Part 2 **29**, L1238 (1990).
[2] K. Pyragas, Phys. Lett. A **170**, 421 (1992).
[3] K. Pyragas and A. Tamasevicius, Phys. Lett. A **180**, 99 (1993).
[4] D.J. Gauthier, D.W. Sukow, H.M. Concannon, and J.E.S. Socolar, Phys. Rev. E **50**, 2343 (1994).
[5] A. Kittel, J. Parisi, K. Pyragas, and R. Richter, Z. Naturforsch. **49A**, 843 (1994).
[6] S. Bielawski, D. Derozier, and P. Glorieux, Phys. Rev. E **49**, R971 (1994).
[7] M. Ye, D.W. Peterman, and P.E. Wigen, Phys. Lett. A **203**, 23 (1995).
[8] A. Babloyantz, C. Lourenco, and J.A. Sepulchre, Physica D **86**, 274 (1995).
[9] A. Namajunas, K. Pyragas, and A. Tamasevicius, Phys. Lett. A **204**, 255 (1995).
[10] T. Hikihara and T. Kawagoshi, Phys. Lett. A **211**, 29 (1996).
[11] Ying Zhang, Jian-Bin Li, Zhi-Ren Zheng, Yun Jiang, and Jin-Yue Gao, Phys. Rev. E **57**, 1611 (1998).
[12] Li Yong-Gui and Zhang Hong-Jun, Acta Phys. Sin. (in Chinese) **32**, 301 (1983).
[13] Jin-Yao Gao, Zhi-Ren Zheng, P. Davis, and Tahito Aida, Opt. Quantum Electron. **31**, 131 (1999).
[14] Zhi-Ren Zheng, Jin-Yao Gao, and Po Dong (unpublished).